

Supporting Information for

**Unlocking Cryptic Metabolites with Mass Spectrometry-Guided Transposon
Mutant Selection**

Aya Yoshimura[†], Brett C. Covington[†], Étienne Gallant[†], Chen Zhang[†], Anran Li[‡], and
Mohammad R. Seyedsayamdost^{†,‡,*}

[†]Department of Chemistry, Princeton University, Princeton, NJ 08544, USA

[‡]Department of Molecular Biology, Princeton University, Princeton, NJ 08544, USA

*Correspondence: mrseyed@princeton.edu

Materials and Methods

Bacterial strains

Burkholderia plantarii ATCC43733 and *Burkholderia gladioli* ATCC10248 were used throughout. Table S1 lists bacterial strains and Tn mutants used in this study.

Materials and General Procedures

All chemicals were purchased from Sigma-Aldrich. Bacterial media were purchased from Becton-Dickinson. Q5 DNA polymerase was obtained from New England Biolabs. PCR purification kits were purchased from Qiagen. EZ-Tn5 <KAN-2> Tnp Transposome Kit was purchased from Epicentre.

LB-MOPS, which consists of LB supplemented with 50 mM MOPS (pH 7.0), was routinely used to culture *B. plantarii* and *B. gladioli*. Other media used are: 8-fold diluted LB medium, M63 medium for creation of site-specific mutants, and M9 minimal medium.

High-resolution (HR) HPLC-MS and HR-tandem HPLC-MS were carried out on a 6540 UHD Accurate Mass Q-tof LC-MS system (Agilent), consisting of a 1260 Infinity Series HPLC system, an automated liquid sampler, a diode array detector, a JetStream ESI source, and the 6540 Series Q-tof or on an Agilent UHD Accurate Mass Q-tof UPLC-MS system, equipped with a 1290 Infinity II series UHPLC, an automated liquid sampler, a diode array detector, a JetStream ESI source, and the 6546 series Q-tof. HPLC purifications were carried out on an Agilent 1260 Infinity Series analytical or preparative HPLC system equipped with a photodiode array detector and an automated fraction collector. NMR spectra were collected at the Princeton Chemistry NMR Core Facility in a Bruker Avance III 800 MHz spectrometer equipped with a ¹H-optimized cryoprobe. Optical density at 600 nm (OD600) was measured using a Synergy H1 microplate reader (Biotek).

Transposon mutagenesis

To create random Tn mutants, *B. plantarii* or *B. gladioli* were plated onto LB-agar plates from frozen stocks, grown overnight at 30°C, and the resulting colonies used to inoculate 14 mL bacterial culture tubes containing 5 mL of LB-MOPS. These were grown overnight, diluted into 20 mL LB-MOPS in a 125 mL Erlenmeyer flask to an initial OD600 of 0.05, cultured for 3 h at 30°C/250 rpm, and pelleted by centrifugation. Cells were washed 3 times with cold 10% glycerol and resuspended at 70 µL 10% glycerol. They were then electroporated with 0.5 µL of the EZ-Tn5 <KAN-2> Tnp at 1500 V for 5 ms, returned to ice for 2 min, grown at 30°C/250 rpm for 2 h, plated on LB plates containing kanamycin (40 µg/mL), and incubated overnight at 30°C.¹ The resulting individual colonies were arrayed into 96-well plates containing 110 µL LB-MOPS, grown overnight at 30°C/250 rpm, then supplemented with 110 µL of 40% glycerol, and the plates were stored at -80°C until further use.

HPLC-MS-Based SOM Analysis

Seventy two randomly selected *B. plantarii* Tn mutants from the 96-well storage stocks were streaked out individually onto LB-agar plates containing kanamycin (40 µg/mL). A single colony from each LB plate was used to inoculate 5 mL of LB-MOPS with kanamycin (40 µg/mL) in a 14 mL culture tube. After growth at 30°C/250 rpm for 1 day, the saturated cultures were used to inoculate 20 mL of LB-MOPS in 125 mL Erlenmeyer flasks to an initial OD600 of 0.05. After growth for 24 h at 30°C/250 rpm, the cells were removed by centrifugation and the supernatant applied directly to a manually-prepared C18 open-column (Phenomenex, 55 µm,

50 mg), which had been washed with MeOH and equilibrated in water. After application of the supernatant, the column was washed with 1 mL each of 0%, 50% and 100% MeOH in water. The 50% MeOH and 100% MeOH fractions were combined and dried *in vacuo*.

The samples were resuspended in 0.2 mL of MeOH, and 2 μ L injected onto a Kinetex column (Phenomenex, 2.6 μ m, 10 x 250 mm) on an Agilent 6540 HPLC-MS system. Elution was carried out with water and MeCN as mobile phases (each containing 0.1% formic acid) and a gradient of 10%-100% MeCN over 20 minutes at 0.5 min/mL. HR-MS data were collected in positive ion mode. For each run, m/z and retention times were extracted and aligned across all 76 samples (72 Tn mutants, 4 wt replicates) using Agilent Profinder v. B.06.00. The threshold parameters were set to an ion count of $\geq 10^5$, yielding 2224 tabulated features (ions with discrete m/z and retention time). These were organized into a 25 x 26 node grid using a self-organizing map package described previously.² The four wt replicates were averaged and 3-times of this composite subtracted from each of the Tn maps. The colored nodes, therefore, in each difference map contain features that are >3-times greater than the corresponding feature in the wt sample. The 72 difference maps thus obtained are shown (Figure S1).

IMS-Based 3D Map Analysis

For IMS screening, the *B. gladioli* Tn mutant library was used to inoculate ten 96-well plates, with each well containing 110 μ L LB-MOPS with kanamycin (40 μ g/mL). After 24 h growth at 30°C/250 rpm, 2 μ L of each well were used to inoculate a second set of ten 96-well plates, with each well containing 110 μ L of LB-MOPS. The plates were incubated for 24 h at 30°C/250 rpm. Then, the cells were removed by centrifugation in a 96-well plate centrifuge, and the supernatant subjected to C18-based solid-phase extraction in a 96-well format (Phenomenex, 33 μ m, 30 mg/well). After application of the supernatant, the column was washed with 0.5 mL each of 0%, 50% and 100% MeOH in water. The 50% MeOH and 100% MeOH fractions were combined and dried *in vacuo*. Each well was resuspended in 20 μ L of 50% MeOH and then imaged using a LAESI DP1000 system (Protea Bioscience) coupled to a LTQ XL mass spectrometer (Thermo). The extension tube connecting the two instruments was kept at 130°C with an external heater, and the sample stage was kept at 10°C during analysis. The sheath-gas flow was set to 2.0 L/h. Eighty laser pulses were applied to each well to ablate samples with an 80% laser energy setting (~850 μ J) and a 10-Hz frequency. A solution of 2:1 MeCN/water with 0.1% acetic acid (v/v) was supplied as the electrospray solution with a syringe pump running at a flow rate of 1 μ L/min.³ The emitter was connected to high-voltage power operating at +4,000 V in positive-ion detection mode. All data were visualized in ProteaPlot software.

After data collection, the signals observed in each well were extracted with GMSU-LAESI software (Gubbs), which yielded all m/z values and the corresponding intensities per well (i.e., per Tn mutant). The data were binned in 1- m/z units for 3D plotting. Signals with an intensity value lower than a set threshold of 2-fold the average wt value were not included in the 3D plots. These data were then visualized using the interactive graphing package plotly in R. Peaks from these 3D maps were visually identified and hits were pursued in HPLC-MS analyses from follow-up flask cultures.

Purification and Structure Elucidation of Haereoplantins and Burrioplantin A

B. plantarii ML939 was streaked out onto an LB-agar plate with kanamycin (40 μ g/mL) and grown at 30°C overnight. The resulting colonies were used to inoculate 5 mL of LB-MOPS containing kanamycin (40 μ g/mL) in a 14 mL culture tube. After growth at 30°C/250 rpm for 24

h, the overnight was used to inoculate 100 mL of LB-MOPS plus kanamycin (40 µg/mL) in a 500 mL Erlenmeyer flask. After growth at 30°C/250 rpm for 24 h, the 100 mL culture was used to inoculate 6 x 4 L Erlenmeyer flasks, each carrying 1 L of 8-fold-diluted LB, to an initial OD₆₀₀ of 0.05. After incubation for 48 h at 30°C/130 rpm, the cells were removed by centrifugation and the supernatant applied directly to a manually-prepared C18 open-column (Phenomenex, 55 µm, 10 g), which had been washed with MeOH and equilibrated in water. After application of the supernatant, the column was washed with 80 mL each of 0%, 30%, 60% and 100% MeOH in water. Each fraction was dried *in vacuo*. Haereoplantins and burrioplantin A were detected in the 60% MeOH fraction. The 60% MeOH fraction was concentrated *in vacuo*, the residue dissolved in a small volume of MeOH and fractionated by HPLC using a preparative Luna Phenyl-Hexyl column (Phenomenex, 5 µm, 21.20 x 250 mm) with H₂O/MeCN containing 0.1% formic acid as mobile phases. Material was eluted with a gradient of 20% MeCN to 100% MeCN over 30 min. Fractions containing haereoplantins and burrioplantin A, as judged by HPLC-MS, were combined and concentrated *in vacuo*. The residue was then chromatographed on a semi-preparative Luna C18 column (Phenomenex, 5 µm, 10 x 250 mm) with H₂O/MeCN containing 0.1% formic acid as mobile phase. Elution was carried out isocratically at 50% MeCN, which separated the six compounds and afforded each in >90% purity.

The structures of haereoplantin A-E and burrioplantin A were determined by analysis of 1D (¹H and ¹³C) and 2D (COSY, NOESY, HSQC and HMBC) NMR spectra and HR-MS data. See Table S3 for molecular formulae and HR-MS data. NMR assignments are listed in Tables S4, S6-S10.

Assignment of absolute configuration was conducted using Marfey's protocol with haereoplantin A and burrioplantin A.⁴ To a solution of haereoplantin A or burrioplantin A (approx. 0.2 mg) was added 6 N HCl (0.2 mL), which was reacted for 24 h at 110 °C. The reaction mixture was dried *in vacuo*. The obtained hydrolysate was dissolved in H₂O (50 µL), to which 1 M NaHCO₃ (20 µL) and L- or D-FDAA (1% w/v in acetone, 100 µL) were added, and the mixture was stirred for 1 h at room temperature. The solution was neutralized with 1 N HCl (20 µL), evaporated, and then dissolved in MeOH. The derivatives were analyzed by HPLC-Qtof-MS. HPLC separation was performed on a Kinetex column (Phenomenex, 2.6 µm, 10 x 250 mm) with a gradient elution of 10% MeCN to 100% MeCN over 45 min (both water and MeCN contained 0.1% formic acid). The result of Marfey's analysis are shown in Table S5.

Purification and Structural Elucidation of Gladiobactin A

B. plantarii ML940 was streaked out onto an LB-agar plate with kanamycin (40 µg/mL) and grown at 30°C overnight. The resulting colonies were used to inoculate 5 mL of LB-MOPS plus kanamycin (40 µg/mL) in a 14 mL culture tube. After growth at 30°C/250 rpm for 24 h, the overnight was used to inoculate 100 mL of LB-MOPS + kanamycin (40 µg/mL) in a 500 mL Erlenmeyer flask. After growth at 30°C/250 rpm for 24 h, the 100 mL culture was used to inoculate 6 x 2 L Erlenmeyer flasks, each carrying 1 L of M9 minimal medium with glycerol (0.2% v/v) as the carbon source. After growth 48 h at 30°C/120 rpm, the cells spun down and the supernatant applied directly to a manually-prepared C18 open-column (Phenomenex, 55 µm, 10 g). The column was washed with 80 mL each of 0%, 30%, 60% and 100% MeOH in water. Each fraction was dried *in vacuo*. Gladiobactin A was detected in the 60% and 100% MeOH fractions. These were combined, concentrated *in vacuo*, the residue dissolved in a small volume of MeOH, and fractionated by HPLC on a preparative Luna C18 column (Phenomenex, 5 µm, 21.20 x 250 mm) with H₂O/MeCN plus 0.1% formic acid as mobile phase. Elution was carried out from 20% MeCN to 100% MeCN over 30 min. Fractions containing gladiobactin A, as judged

by HPLC-MS, were combined, concentrated *in vacuo*, dissolved in MeOH, and chromatographed on a semi-preparative Luna C18 column (Phenomenex, 5 μ m, 10 x 250 mm) with H₂O/MeCN plus 0.1% formic acid as mobile phase. Elution was carried out isocratically with 50% MeCN and yielded pure gladiobactin A. The structure of gladiobactin A was determined by analysis of ¹H, COSY, TOCSY, HSQC and HMBC spectra and HR-MS data (see Tables S3, S13). Absolute configurations were determined using Marfey's method and the appropriate standards as described above for haereoplantin A (Table S5).

Creation of Site-Specific Deletion Mutants in *B. plantarii*

All deletion mutants were constructed by natural competence transformation with linear DNA fragments, which were created by joining three fragments corresponding to the upstream and downstream 1 kb regions flanking the gene to be deleted and the tetracycline resistance marker (*tet*). Competent *B. plantarii* cells were generated by growing the bacteria overnight in a 5 mL low-salt LB-medium at 37°C/200 rpm. The overnight culture was used to inoculate 3 mL of M63 medium in a 50 mL Erlenmeyer flask grown at 37°C/200 rpm. After 27 h, the cells were pelleted by centrifugation at 16,000g for 3 min, and the supernatant was discarded. The cells were resuspended in 50 μ L of M63 medium in a sterile 1.5 mL Eppendorf tube. ~500 ng of linear DNA fragment was mixed with the cells by gently tapping the tube, and the resulting mixture was incubated at room temperature for 30 min. The mixture was then transferred into 2-3 mL of M63 medium in a 14 mL culture tube and grown at 37°C/200 rpm overnight. The overnight culture was pelleted by centrifugation and the cells were resuspended in 50 μ L M63 medium and plated on LB agar supplemented tetracycline (20 μ g/mL). The plate was then incubated at 37°C for 24 h or until colonies developed. The mutant colonies were verified by PCR and sequencing. Primers used in this study are listed in Table S1.

Identification of Tn5 Insertion Sites

The desired mutant was cultured in 5 mL of LB-MOPS overnight, as described above, and then pelleted by centrifugation. Genomic DNA was isolated using the Promega Wizard Genomic DNA Purification Kit. Arbitrary PCR was then carried as previously reported without modifications⁵ to amplify the Tn5-adjacent regions, which were sequenced at Genewiz. The insertion sites were identified using the publically available genome sequence of *B. plantarii*.

Spermidine Supplementation Experiments

A 5 mL overnight culture of *B. gladioli* was prepared in LB-MOPS in a 14 mL culture tube, as described above, and incubated at 30°/250 rpm. The overnight culture was diluted into 20 mL of M9 medium plus glycerol (0.2% v/v) and supplemented with increasing concentrations of spermidine (0-3.2mM) in a 125 mL Erlenmeyer flask. The cultures were grown at 30°C/200 rpm for 48 hours and OD600 was subsequently measured. Supernatants from the cultures were filtered and analyzed on an Agilent UHD Accurate Mass UPLC-MS system with the 6454 series Q-tof. The samples were resolved on an Agilent Poroshell 120 EC-C18 column (1.9 μ m, 2.1 x 50 mm) at 0.5 mL/min using H₂O/MeCN (+0.1% formic acid) as mobile phase. Elution was carried out isocratically for 1.5 min at 20% MeCN, followed by a gradient from 15-100% MeCN over 3.5 min. The extracted ion chromatogram for gladiobactin A and ferric-gladiobactin A ($[M+H]^+$ =1105.5848 and $[M-2H+Fe]^+$ =1158.4967, respectively) was integrated and normalized by OD600. Results from two independent biological replicates were averaged to give the values in Fig. 6C.

SI Tables

Table S1. Strains (top) and primers (bottom) used in this study.

Bacterial strain	Description	Source
<i>B. plantarii</i> ATCC 43733	wild-type	ATCC
<i>B. gladioli</i> ATCC 10248	wild-type	ATCC
<i>B. plantarii</i> ML939	<i>helicase::Tn5</i>	This study
<i>B. plantarii</i> ML943	<i>helicase::tet</i>	This study
<i>B. plantarii</i> ML946	<i>helicase::Tn5, hptC::tet</i>	This study
<i>B. plantarii</i> ML944	<i>helicase::Tn5, bptE::tet</i>	This study
<i>B. gladioli</i> ML940	<i>potF::Tn5</i>	This study

Primer name	Primer Sequence	Purpose
NRPS_F1	GATCGTCAACGGCGAGAGAGCTACG	Construction of <i>B. plantarii</i> ML946
NRPS_R1	AGGAGGTTCCGACGGGCAAGGCACTGCG	
NRPS_Ftet	GCCCGTCGGAACCTCCTTTAACTCCTCAAAACGAAC	
NRPS_Rtet	TAGCCGTCGGGAGTGGTGAATCCGTTAGCGAGG	
NRPS_F2	GATTCACCACTCCCGACGGCTATCTGGCGCGG	
NRPS_R2	CCGGCTTGTCGAAATCGAGTCC	
helicase_F1	GCGATGAGGGCGACCGAGCA	Construction of <i>B. plantarii</i> ML943
helicase_R1	GGAGGTTCCCGGTGGGTGAAACGTCGGCG	
helicase_Ftet	CACCCACGGGAACCTCCTTTAACTCCTCAAAACGAAC	
helicase_Rtet	AATGTCGGCGGTGGTGAATCCGTTAGCGAGGTGCC	
helicase_F2	GGATTCACCACCGCCGACATTTACGATGCG	
helicase_R2	GCACCTTGCCGCCATGTGG	
Big_NRPS_F1	CAGGTTGCCCGCCCCATCG	Construction of <i>B. plantarii</i> ML944
Big_NRPS_R1	TTAAAGGAGGTTCCGCGCTCTCTCAATTCGCAATTCCATG	
Big_NRPS_Ftet	GAGAGAGCGCGGAACCTCCTTTAACTCCTCAAAACGAA	
Big_NRPS_Rtet	GCATGCACATTGGAGTGGTGAATCCGTTAGCAGG	
Big_NRPS_F2	ATTCACCACTCCAATGTGCATGCGGCTGTAACCGTTTC	
Big_NRPS_R2	TCGCCACCCAGCCTGACTC	

Table S2. AntiSMASH results of the *B. plantarii* genome.

Cluster	Type	Most similar known cluster	Similarity
1	NRPS-T1PKS	oxalomycin	9%
2	NRPS-T1PKS	glidobactin	15%
3	betalactone-terpene	barbamide	33%
4	NRPS-homoserine lactone	bactobolin	9%
5	siderophore	staphylobactin	18%
6	homoserine lactone		
7	phosphonate	phosphinothricin tripeptide	6%
8	bacteriocin		
9	NRPS-betalactone	fragin	62%
10	NRPS	gramibactin	40%
11	NRPS	rhizomide	100%
12	betalactam		
13	terpene		
14	terpene		
15	bacteriocin		
16	T1PKS	capsular polysaccharide	25%
17	homoserine lactone		
18	NRPS	lysobactin	3%
19	T2PKS	APE Vf	30%
20	bacteriocin		
21	NRPS-T1PKS		
22	NRPS	pyochelin	60%
23	CDPS	bicyclomycin	75%
24	terpene		
25	NRPS		

Table S3. AntiSMASH results of the *B. gladioli* genome.

Cluster	Type	Most similar known cluster	Similarity
1	homoserine lactone		
2	T1PKS	lipopolysaccharide	5%
3	NRPS	sulfazecin	100%
4	NRPS		
5	T1PKS-NRPS	orfamide	30%
6	terpene	lasalocid	7%
7	transAT-PKS	etnangien	68%
8	NRPS	rhizomide	100%
9	phosphonate	phosphinothricintripeptide	6%
10	bacteriocin		
11	NRPS	pyoverdine	1%
12	NRPS	gramibactin	46%
13	NRPS	rhizomide	100%
14	T1PKS	lactimidomycin	66%
15	terpene		
16	terpene		
17	terpene	desotamide	9%
18	NRPS	icosalide	100%
19	betalactone-terpene	barbamide	41%

Table S4. Features observed in the four regions of interest upon HPLC-MS-based SOM analysis of *B. plantarii* Tn mutants. The locations of the four regions are shown in the map to the bottom left. The features in each region of interest (ROI) are tabulated. The feature ID is comprised of “M” followed by the *m/z* of the compound and “T” followed by the feature retention time, both of which are determined by the MassHunter Profinder feature extraction algorithm.

ROI 1		ROI 2		ROI 3		ROI 4	
Feature ID	Fold Change	Feature ID	Fold Change	Feature ID	Fold Change	Feature ID	Fold Change
M301.2T9.8	6	M603.3T4.8	>100	M284.1T12.4	10	M219.1T10.9	5
M414.2T2.9	>100			M385.2T4.7	8	M242.1T2.5	5
M470.2T5.1	>100			M402.2T2.9	53	M628.3T2.7	6
M472.2T5.4	>100			M411.2T3.1	10	M809.4T10.2	4
M477.2T4.4	>100			M508.2T4.4	9	M1021.5T9.6	5
M497.2T3.8	15			M545.2T2.7	7	M1105.5T9.9	3
M528.2T3.1	>100			M627.3T6	14		
M542.2T3.2	7			M635.3T2.8	14		
M560.2T5.7	>100			M821.4T9.1	2		
M578.2T5	>100			M1014.5T3	6		
M649.3T5.7	>100						
M764.3T3.4	58						
M1103.7T8.3	>100						

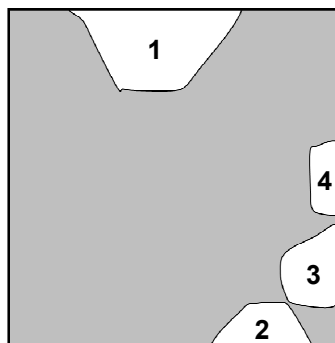
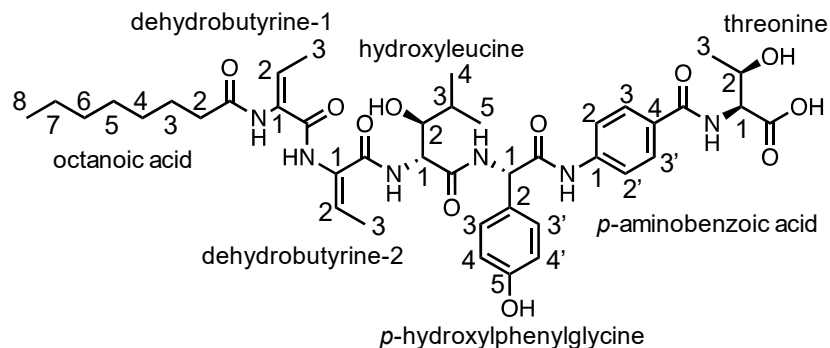


Table S5. Observed and calculated m/z and molecular formulae for metabolites identified in this work.

Compound	[M+H]⁺_{calc}	[M+H]⁺_{obs}	Δppm	Molecular formula
Haereoplatin A	809.4080	809.4068	1.5	C ₄₁ H ₅₆ N ₆ O ₁₁
Haereoplatin B	837.4393	837.4360	3.9	C ₄₃ H ₆₀ N ₆ O ₁₁
Haereoplatin C	793.4131	793.4112	2.4	C ₄₁ H ₅₆ N ₆ O ₁₀
Haereoplatin D	773.4444	773.4423	2.7	C ₃₉ H ₆₀ N ₆ O ₁₀
Haereoplatin E	708.3603	708.3590	1.8	C ₃₇ H ₄₉ N ₅ O ₉
Burrioplatin A	1021.5241	1021.5221	2.0	C ₅₁ H ₇₂ N ₈ O ₁₄
Gladiobactin A	1105.5848	1105.5857	0.8	C ₄₅ H ₈₀ N ₁₄ O ₁₈
Icosalide A	713.4695	713.4689	0.8	C ₃₆ H ₆₄ N ₄ O ₁₀
Icosalide B	685.4382	685.4370	1.8	C ₃₄ H ₆₀ N ₄ O ₁₀
Gladiolin	779.5304	779.5296	1.0	C ₄₄ H ₇₄ O ₁₁

Table S6. NMR assignments for haereoplatin A in DMSO-*d*₆ from *N*- to *C*-terminus. The structure and numbering scheme for haereoplatin A are shown above the table.



Residue	Position	¹³ C	¹ H (mult., <i>J</i> in Hz)
octanoic acid	C=O	172.7	
	2	34.8	2.18 (m)
	3-7	21.7-31.6	1.10-1.54
	8	13.7	0.81
dehydrobutyrine-1	C=O	163.9	
	1	131.3	
	2	118.7	5.57 (q, 7.0)
	3	12.5	1.72 (d, 7.1)
	NH		10.01 (s)
dehydrobutyrine-2	C=O	163.8	
	1	129.2	
	2	127.5	5.79 (q, 7.1)
	3	13.1	1.92 (d, 7.1)
	NH		9.78 (s)
hydroxyleucine	C=O	170.5	
	1	55.7	4.50 (dd, 3.0, 9.0)
	2	76.3	3.58 (m)
	3	30.1	1.63 (m)
	4	18.7	0.91
	5	18.9	0.79
	OH		4.75 (d, 8.1)
NH		7.85 (d, 8.7)	

<i>p</i> -hydroxyphenylglycine	C=O	169.3	
	1	56.8	5.48 (d, 7.5)
	2	127.7	
	3, 3'	128.6	7.26 (d, 8.6)
	4, 4'	114.9	6.68 (d, 8.6)
	5	157.1	
	NH		8.25 (d, 7.6)
<i>p</i> -aminobenzoic acid	C=O	164.4	
	1	141.2	
	2, 2'	118.4	7.72 (d, 8.6)
	3, 3'	127.3	7.64 (d, 8.6)
	4	129.4	
	NH		10.15 (s)
threonine	C=O	171.9	
	1	56.9	3.94 (m)
	2	65.5	3.96 (m)
	3	18.7	0.91
	NH		7.62 (d, 5.8)

Table S7. Marfey's analysis of haereoplantin A, burrioplantin A and gladiobactin A.

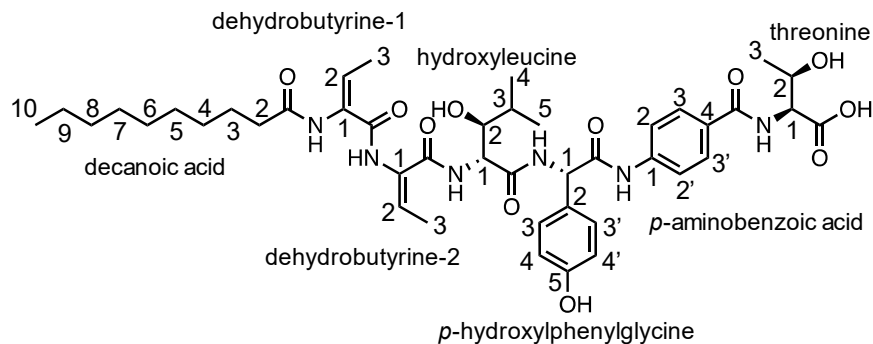
Haereoplantin A	Rt, hydrolyzed haereoplantin A		Rt, standard L-amino acid	Stereo-chemistry
	L-FDAA	D-FDAA	L-FDAA	
(2R,3S)-hydroxyleucine	35.2	30.3	35.2 ^a	2R, 3S
<i>p</i> -hydroxyphenylglycine	40.9	41.7	40.9	L
threonine	23.1	26.6	23.1	L

^a(2R,3S)-hydroxyleucine was used as standard

Burrioplantin A	Rt, hydrolyzed burrioplantin A		Rt, standard L-amino acid	Stereo-chemistry
	L-FDAA	D-FDAA	L-FDAA	
serine	22.5	22.1	22.1	D
alanine	27.2	30.1	27.2	L
<i>p</i> -hydroxyphenylglycine	41.4	40.9	40.9	D
phenylalanine	37.9	40.2	37.9	L
homoserine	23.1	26.6	23.1	L
proline	28.2/29.4	28.2/29.4	28.2	D + L

Gladiobactin A	Rt, hydrolyzed gladiobactin A		Rt, standard L-amino acid	Stereo-chemistry
	L-FDAA	D-FDAA	L-FDAA	
lysine	38.7	39.7	38.7	L
ornithine	36.8	34.8	-	L
β -hydroxyaspartic acid	22.7	21.6	-	L-erythro
serine	22.1/22.5	22.1/22.5	-	D+L
5-hydroxynorvaline	25.5	24.6	-	D
proline	29.3	28.1	28.1	D

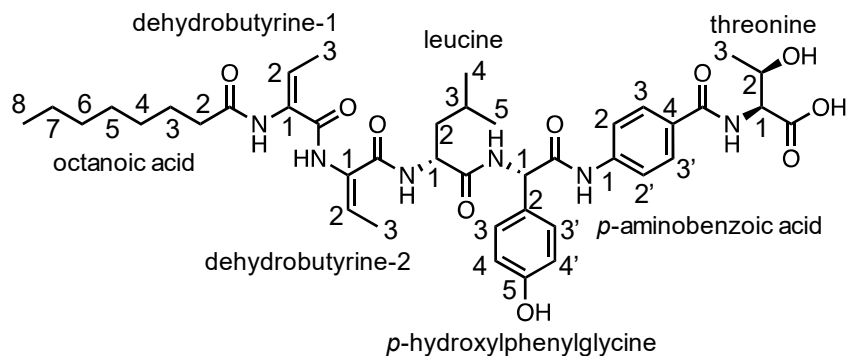
Table S8. NMR assignments for haereoplantin B in DMSO-*d*₆ from N- to C-terminus. The structure and numbering scheme for haereoplantin B are shown above the table.



Residue	Position	¹³ C	¹ H (mult., J in Hz)
decanoic acid	C=O	ND	
	2	ND	2.18 (m)
	3-9	ND	1.14-1.54
	10	ND	0.79
dehydrobutyryne-1	C=O	ND	
	1	ND	
	2	ND	5.57 (q, 7.9)
	3	12.2	1.72 (d, 7.2)
	NH		10.03 (s)
dehydrobutyryne-2	C=O	ND	
	1	ND	
	2	ND	5.78 (q, 7.4)
	3	13.0	1.92 (d, 7.6)
	NH		9.79 (s)
hydroxy-leucine	C=O	ND	
	1	ND	4.50 (dd, 3.3, 8.6)
	2	ND	3.57 (m)
	3	ND	1.62 (m)
	4	18.6	0.91
	5	18.7	0.76
	OH		4.76 (d, 9.2)
NH		7.86 (d, 9.0)	

<i>p</i> -hydroxyphenylglycine	C=O	ND	
	1	ND	5.47 (d, 7.4)
	2	ND	
	3, 3'	128.4	7.25 (d, 8.4)
	4, 4'	114.	6.68 (d, 8.3)
	5	ND	
	NH		8.23 (d, 7.8)
<i>p</i> -aminobenzoic acid	C=O	ND	
	1	ND	
	2, 2'	127.1	7.71 (d, 9.2)
	3, 3'	118.4	7.64 (d, 9.1)
	4	ND	
	NH		10.15 (s)
threonine	C=O	ND	
	1	ND	3.94 (m)
	2	ND	3.94 (m)
	3	ND	0.91
	NH		7.61 (d, 5.1)

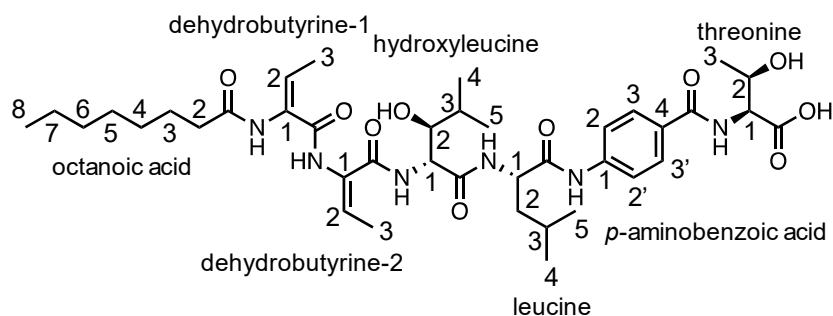
Table S9. NMR assignments for haereoplantin C in DMSO-*d*₆ from N- to C-terminus. The structure and numbering scheme for haereoplantin C are shown above the table.



Residue	Position	¹³ C	¹ H (mult., J in Hz)
octanoic acid	C=O	ND	
	2	34.4	2.19 (m)
	3-7	21.6-32.2	1.11-1.57
	8	13.4	0.80
dehydrobutyrine-1	C=O	ND	
	1	ND	
	2	117.7	5.51 (q, 7.0)
	3	12.2	1.71 (d, 7.3)
	NH		9.91 (s)
dehydrobutyrine-2	C=O	ND	
	1	ND	
	2	127.7	5.77 (q, 7.0)
	3	12.9	1.93 (d, 7.3)
	NH		9.79 (s)
leucine	C=O	ND	
	1	51.2	4.24 (m)
	2	39.3	1.73 (m), 1.52 (m)
	3	23.6	1.65 (m)
	4	20.6	0.81
	5	22.6	0.86
p-hydroxylphenylglycine	NH		8.13 (d, 7.7)
	C=O	ND	

<i>p</i> -aminobenzoic acid	1	56.6	5.42 (d, 7.5)
	2	ND	
	3, 3'	128.4	7.27 (d, 9.0)
	4, 4'	114.6	6.68 (d, 8.6)
	5	ND	
	NH		8.18 (d, 7.7)
	C=O	ND	
	1	ND	
threonine	2, 2'	127.1	7.71 (d, 8.8)
	3, 3'	118.1	7.65 (d, 8.8)
	4	ND	
	NH		10.24 (s)
	C=O	ND	
	1	56.7	3.95 (m)
	2	65.3	3.95 (m)
	3	18.4	0.91
NH		7.61 (d, 5.0)	

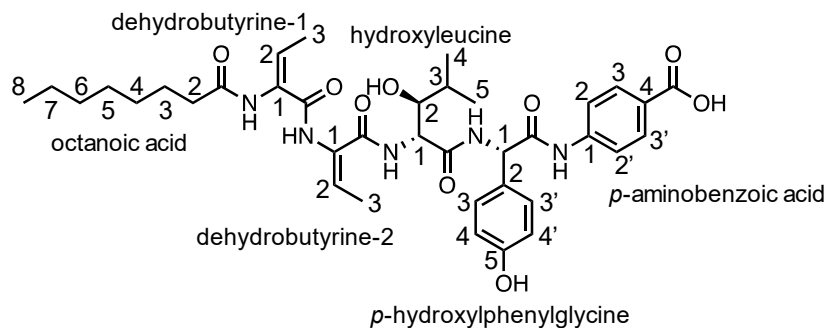
Table S10. NMR assignments for haereoplatin D in DMSO-*d*₆ from N- to C-terminus. The structure and numbering scheme for haereoplatin D are shown above the table.



Residue	Position	¹³ C	¹ H (mult., J in Hz)
octanoic acid	C=O	ND	
	2	34.9	2.14 (m)
	3-7	21.8-31.1	1.12-1.50
	8	13.7	0.80
dehydrobutyrine-1	C=O	ND	
	1	ND	
	2	119.1	5.60 (q, 7.2)
	3	12.5	1.75 (d, 7.3)
	NH		10.10 (s)
dehydrobutyrine-2	C=O	ND	
	1	ND	
	2	125.5	5.75 (q, 7.4)
	3	12.9	1.90 (d, 7.3)
	NH		9.96 (s)
hydroxyleucine	C=O	ND	
	1	55.8	4.43 (m)
	2	76.1	3.62 (m)
	3	30.3	1.63 (m)
	4	18.8	0.95
	5	18.7	0.80
	OH		5.04 (d, 7.5)
NH		7.87 (d, 8.7)	

leucine	C=O	ND	
	1	52.2	4.35 (m)
	2	ND	1.58 (m)
	3	23.7	1.66 (m)
	4	20.9	0.83
	5	22.9	0.86
<i>p</i> -aminobenzoic acid	NH		8.01 (d, 7.9)
	C=O	ND	
	1	ND	
	2, 2'	118.4	7.66 (d, 9.0)
	3, 3'	127.1	7.71 (d, 9.1)
	4	ND	
threonine	NH		9.55 (s)
	C=O	ND	
	1	56.9	3.95 (m)
	2	65.4	3.95 (m)
	3	18.6	0.91
	NH		7.63 (d, 5.2)

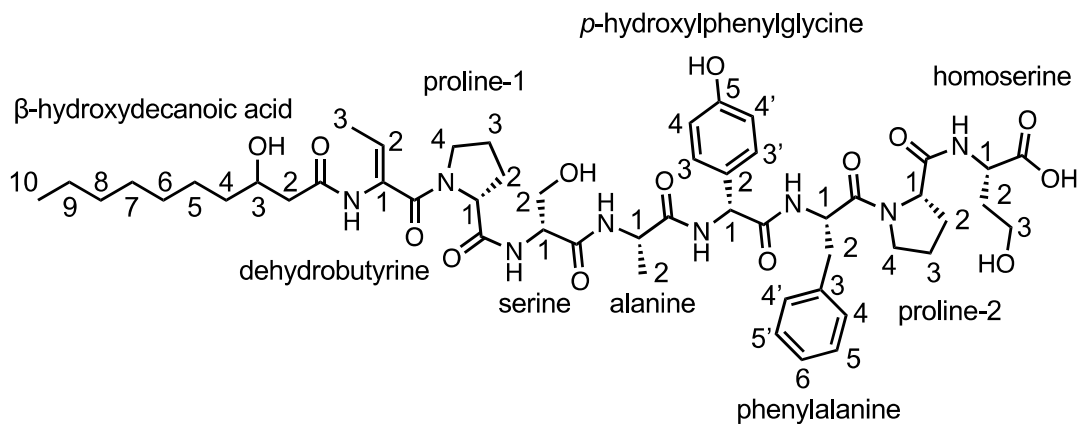
Table S11. NMR assignments for haereoplatin E in DMSO-*d*₆ from *N*- to *C*-terminus. The structure and numbering scheme for haereoplatin E are shown above the table.



Residue	Position	¹³ C	¹ H (mult., <i>J</i> in Hz)
octanoic acid	C=O	ND	
	2	34.5	2.19 (m)
	3-7	20.6-31.5	1.15-1.54
	8	13.5	0.81
dehydrobutyrine-1	C=O	ND	
	1	ND	
	2	118.5	5.57 (q, 7.4)
	3	12.3	1.72 (d, 7.2)
	NH		10.04 (s)
dehydrobutyrine-2	C=O	ND	
	1	ND	
	2	127.3	5.79 (q, 7.4)
	3	13.0	1.92 (d, 7.5)
	NH		9.78 (s)
hydroxyleucine	C=O	ND	
	1	55.5	4.50 (dd, 3.5, 8.9)
	2	76.0	3.57 (m)
	3	29.8	1.63 (m)
	4	18.7	0.78
	5	18.5	1.75
	OH		4.76 (d, 8.5)
NH		7.88 (d, 8.8)	

<i>p</i> -hydroxyphenylglycine	C=O	ND	
	1	56.6	5.46 (d, 8.0)
	2	ND	
	3, 3'	128.3	7.25 (d, 8.7)
	4, 4'	114.5	6.67 (d, 8.6)
	5	ND	
<i>p</i> -aminobenzoic acid	NH		8.22 (d, 7.5)
	C=O	ND	
	1	ND	
	2, 2'	129.2	7.75 (d, 8.4)
	3, 3'	117.5	7.46 (d, 8.3)
	4	ND	
	NH		9.92 (s)

Table S12. NMR assignments for burrioplantin A in DMSO-*d*₆ from N- to C-terminus. The structure and numbering scheme for burrioplantin A are shown above the table.



Residue	Position	¹³ C	¹ H (mult., J in Hz)
β -hydroxydecanoic acid	C=O	171.6	
	2	42.8	2.30 (m)
	3	67.1	3.78 (m)
	4-9	21.9-37.0	1.19-1.40
	10	13.7	0.86 (t, 6.5)
dehydrobutyrine	C=O	166.97	
	1	131.9	
	2	119.2	5.55 (q, 7.1)
	3	11.8	1.68 (d, 6.6)
	NH		9.76 (s)
proline-1	C=O	171.4	
	1	60.2	4.25
	2	29.1	2.14, 1.77
	3	24.3	1.82, 1.75
	4	48.8	3.60, 3.45
serine	C=O	169.6	
	1	55.8	4.18
	2	61.3	3.64
	OH		4.84
	NH		7.80 (d, 7.7)

alanine	C=O	171.5	
	1	48.5	4.20
	2	17.5	1.18 (d, 7.0)
	NH		7.59 (d, 6.2)
<i>p</i> -hydroxyphenylglycine	C=O	169.9	
	1	54.4	5.40 (d, 8.5)
	2	129.1	6.51 (d, 7.9)
	3, 3'	114.3	6.84 (d, 7.9)
	4, 4'	127.1	
	5	156.3	
	NH		8.08 (d, 8.3)
phenylalanine	C=O	170.1	
	1	52.8	4.53
	2	36.5	2.98, 2.75
	3	137.6	
	4, 4', 5, 5', 6	125.9-129.0	7.12-7.20
	NH		8.82 (d, 7.7)
proline-2	C=O	172.5	
	1	59.3	4.48
	2	28.4	1.93, 1.99
	3	24.3	1.90
	4	46.5	3.63
homoserine	C=O	173.1	
	1	48.8	4.31
	2	33.8	1.70, 1.81
	3	56.8	3.39, 3.44
	NH		8.13 (d, 7.2)

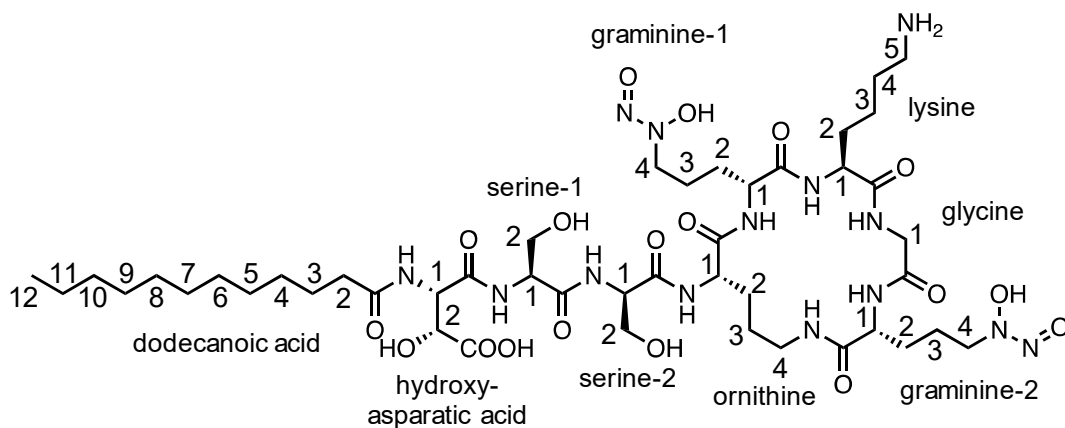
Table S13. Predicted functions for proteins in the *hpt* gene cluster.

Protein	Putative function	NCBI accession
HptA	VOC family protein	WP_082465193.1
HptB	Aminodeoxychorismate synthase	WP_055138301.1
HptC	NRPS (C-A-T-C-A-T-C-A-T-C-A-T-C-A-T-TE)	WP_055138302.1
HptD	Cupin-like domain containing protein	WP_158512003.1
HptE	MFS efflux pump	WP_042624381.1
HptF	ABC transporter permease	WP_042624382.1
HptG	ABC transporter permease	WP_042624383.1
HptH	ABC transporter substrate binding protein	WP_055138304.1

Table S14. Predicted functions for proteins in the *bpt* gene cluster.

Protein	Putative function	NCBI accession
BptA	four helix bundle domain-containing protein	WP_055140513.1
BptB	Glycosyltransferase	WP_055140514.1
BptC	Thioredoxin family protein	WP_055140515.1
BptD	DUF1223 domain containing protein	WP_055140516.1
BptE	NRPS (C-A-T-C-A-T-C-A-T-C-A-T-C-A-T-C-A-T-C-A-T-TE)	WP_055140517.1
BptF	Porin	WP_042628186.1
BptG	methyl-accepting chemotaxis protein	WP_055140518.1
BptH	Hypothetical	WP_055140519.1
BptI	MFS transporter	WP_055140520.1
BptJ	phytanoyl-CoA dioxygenase family protein	WP_055140521.1
BptK	5-enolpyruvylshikimate-3-phosphate synthase	WP_042628191.1

Table S15. NMR assignments for gladiobactin in DMSO-*d*₆ from N- to C-terminus. The structure and number scheme for the compound is shown above the table.



Residue	Position	¹³ C	¹ H (mult., J in Hz)
dodecanoic acid	C=O	171.3	
	2	34.9	2.06 (m)
	3-11	21.0-32.1	1.09-1.48
	12	13.8	0.85 (t, 7.1)
hydroxyasparatic acid	C=O	171.1	
	1	57.1	3.77 (dd, 5.4, 10.2)
	2	73.0	3.73 (m)
	COOH	177.6	
	NH		7.62 (d, 5.2)
serine-1	C=O	171.6	
	1	55.5	3.90 (m)
	2	61.1	3.66, 3.73 (m)
	OH		4.99
	NH		6.82 (d, 6.7)
serine-2	C=O	169.6	
	1	56.9	3.93 (m)
	2	59.4	3.60, 4.07 (m)
	NH		8.94 (d, 5.6)
ornithine	C=O	170.7	
	1	55.1	3.54 (m)

	2	26.9	1.35, 1.44 (m)
	3	24.3	1.17 (m)
	4	36.2	2.66, 3.46 (m)
	NH		6.14 (d, 10)
	NH		6.72 (d, 4.3)
graminine-1	C=O	172.2	
	1	50.7	4.24 (m)
	2	27.5	1.15, 1.41 (m)
	3	22.5	1.59, 1.83 (m)
	4	55.9	4.13 (m)
	NH		6.75 (d, 7.9)
lysine	C=O	173.5	
	1	54.6	3.69 (m)
	2	29.9	1.57, 1.63 (m)
	3	21.8	1.28, 1.41 (m)
	4	27.7	1.52 (m)
	5	38.3	2.71 (m)
	NH		8.54 (s)
glycine	C=O	172.5	
	1	42.4	3.48, 3.72 (m)
	NH		8.85 (m)
graminine-2	C=O	168.8	
	1	54.1	4.00 (m)
	2	27.6	1.55, 2.25 (m)
	3	21.7	1.82, 2.00 (m)
	4	57.9	4.02, 4.58 (m)
	NH		7.58 (d, 8)

Table S16. Predicted functions for proteins in the *gld* gene cluster.

Protein	Putative function	NCBI accession
GldA	MbtH family protein	WP_013690465.1
GldB	Thioesterase	WP_036056054.1
GldC	TauD family dioxygenase	WP_036056055.1
GldD	NRPS (C-A-T-E-C-A-T-C-A-T)	WP_036056057.1
GldE	NRPS (C-A-T-E-TE)	WP_052710563.1
GldF	ABC transporter, ATP-binding	WP_017922115.1
GldG	ABC transporter, iron-compound binding	WP_036056058.1
GldH	ABC transporter permease	WP_036056059.1
GldI	TonB-dependent siderophore receptor	WP_036056060.1
GldJ	Peptide synthetase, GrbD homolog	WP_036056061.1
GldK	Yqcl/YcgG protein, GrbE homolog	WP_036029368.1
GldL	NRPS (FAL-T-C-A-T-C-A-T)	WP_036056063.1
GldM	NRPS (C-A-T-E-C-A-T)	WP_036056065.1
GldN	ABC transporter	WP_036056067.1

SI Figures

Figure S1. All 72 differential self-organizing maps from HPLC-MS analysis of 72 *B. plantarii* Tn mutants. Red and yellow colored nodes in each of the difference maps contain features that are >3-fold more abundant than the wild-type average.

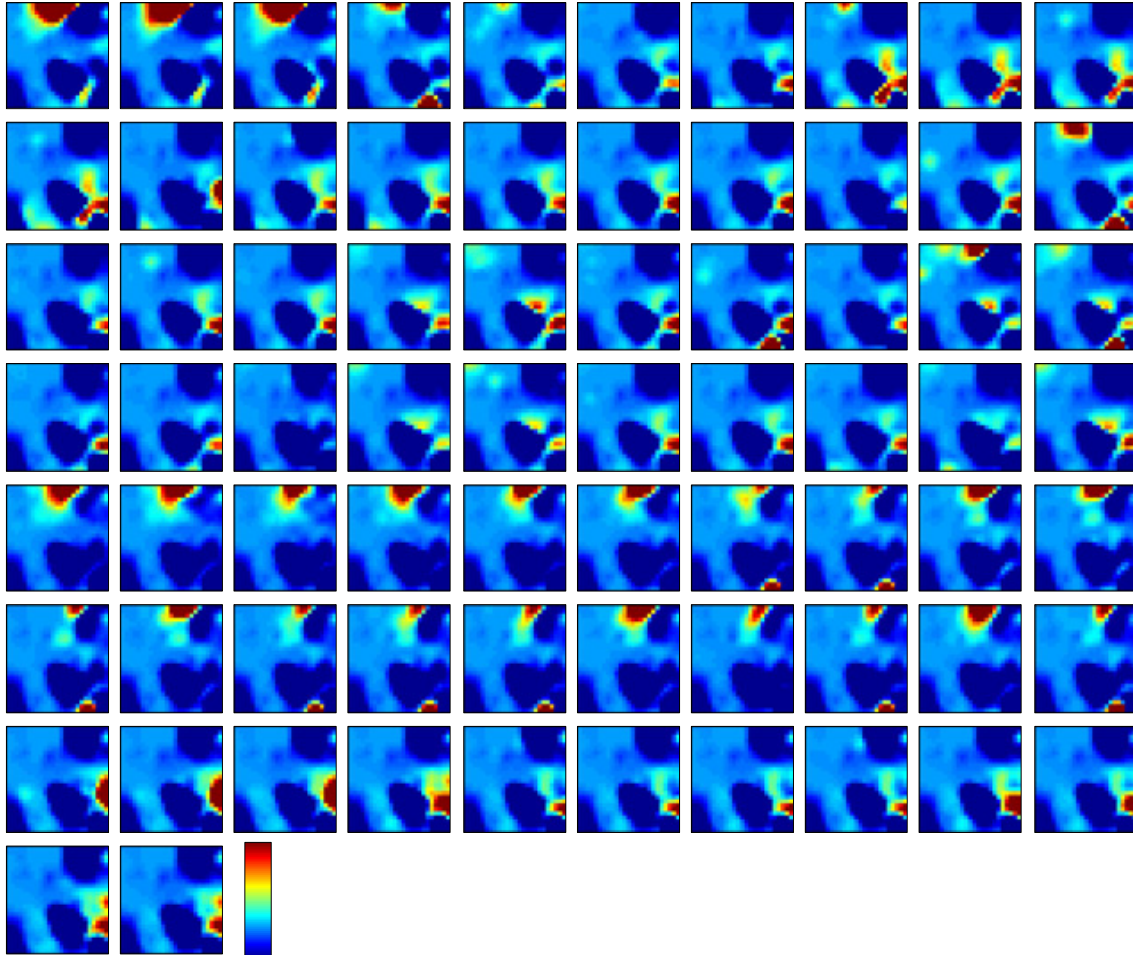


Figure S2. 800 MHz NMR spectra of haereoplanin A in DMSO-*d*₆. Shown are ¹H, ¹³C, COSY, HSQC, HMBC, and NOESY spectra.

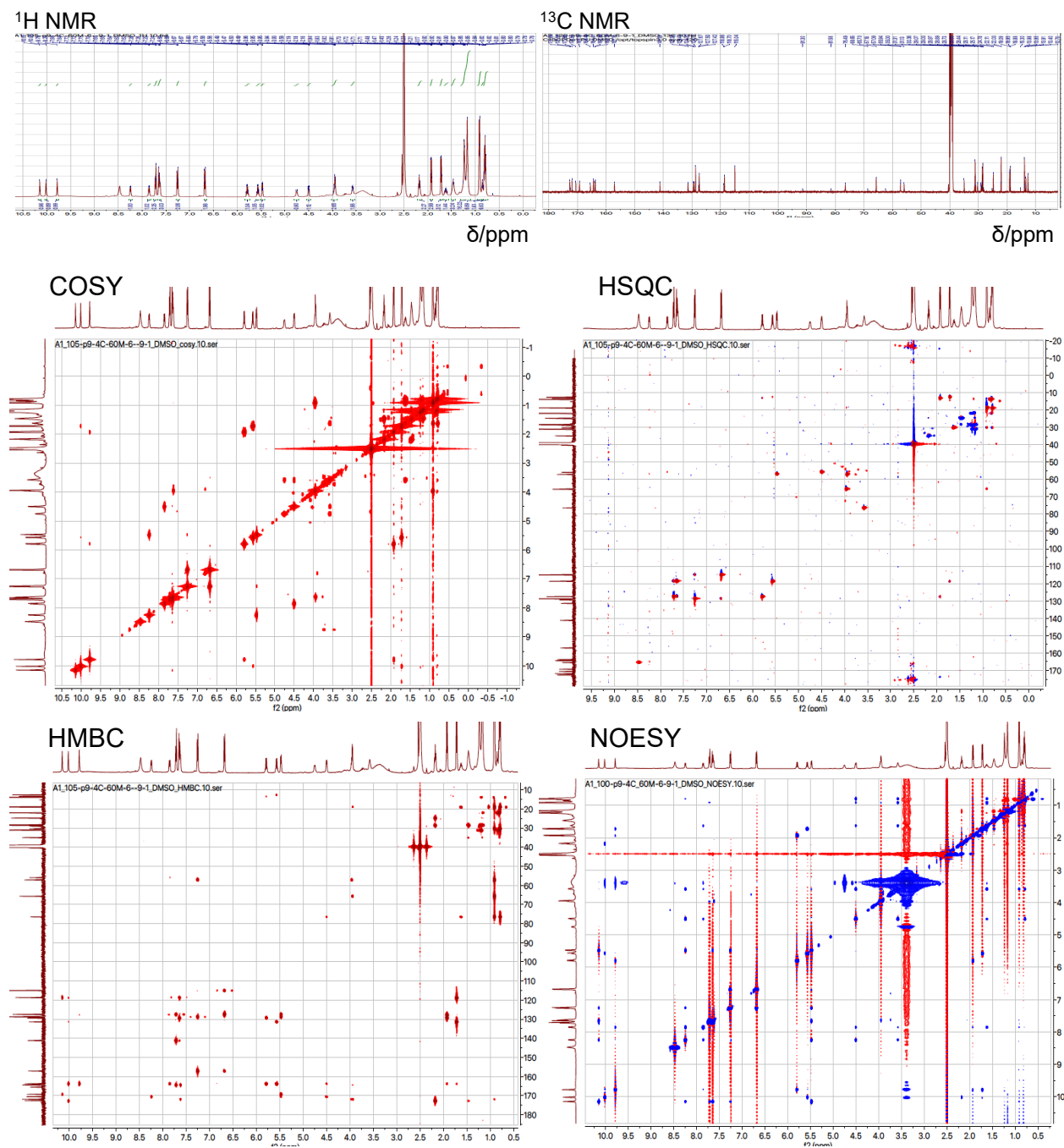
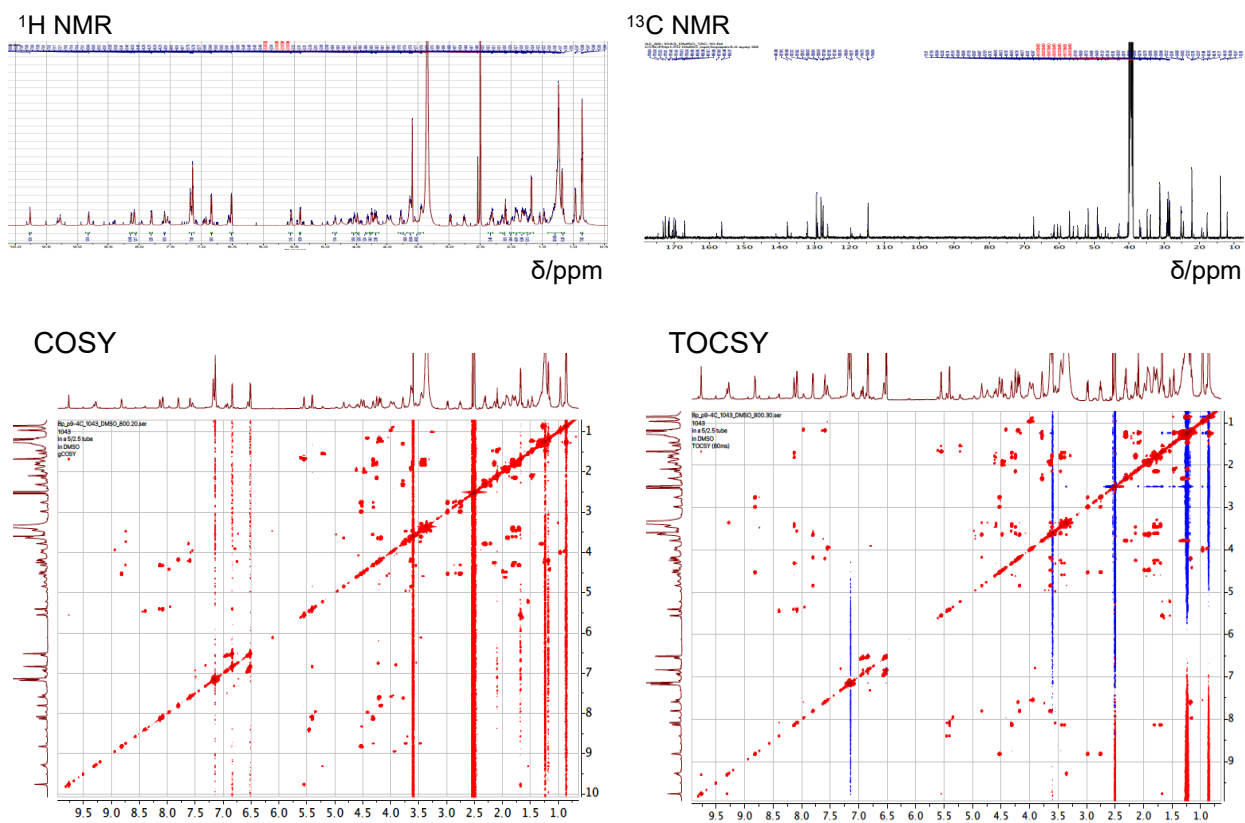


Figure S3. 800 MHz NMR spectra of burrioplantin A in DMSO-*d*₆. Shown are ¹H, ¹³C, COSY, TOCSY (page S31) and HSQC, HMBC, and ROESY spectra (page S32).



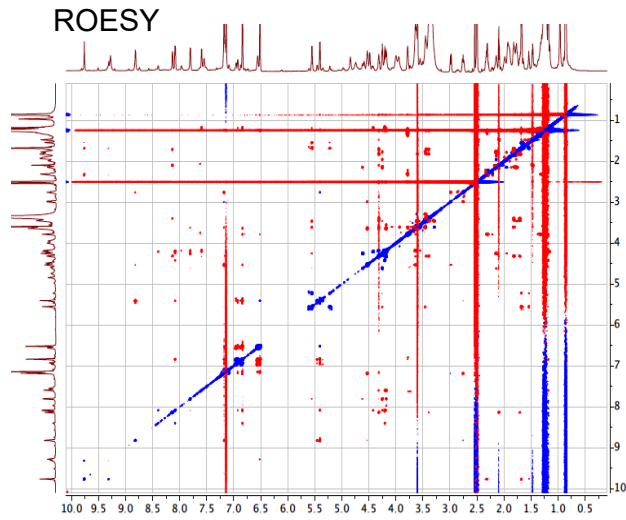
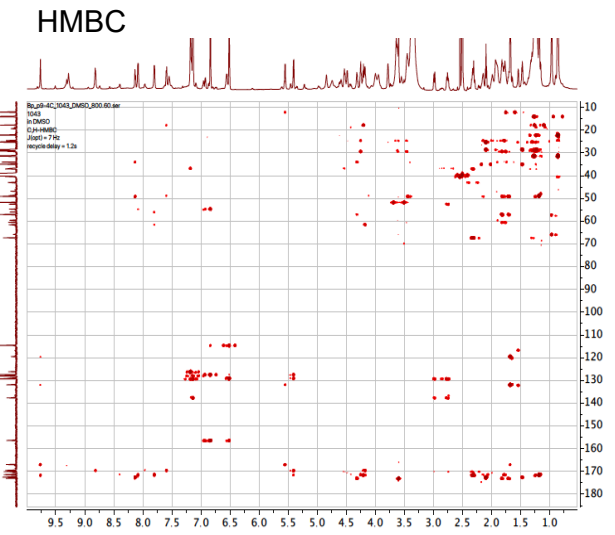
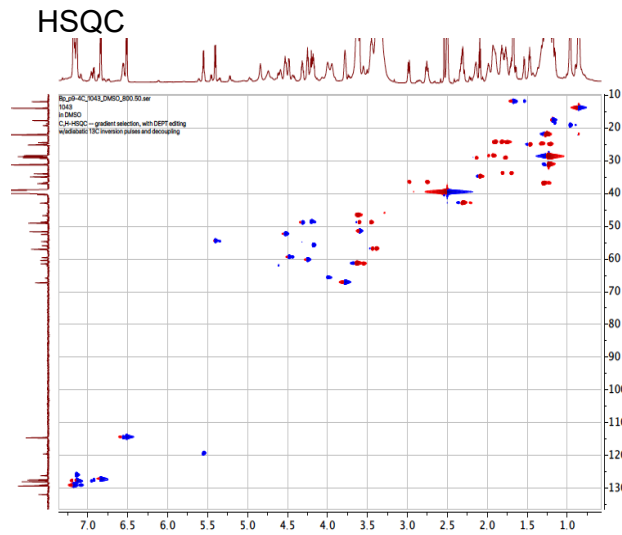


Figure S4. Proposed biosynthetic pathway for haereoplantin A (top) and burrioplantin A (bottom). See Tables S13-S14.

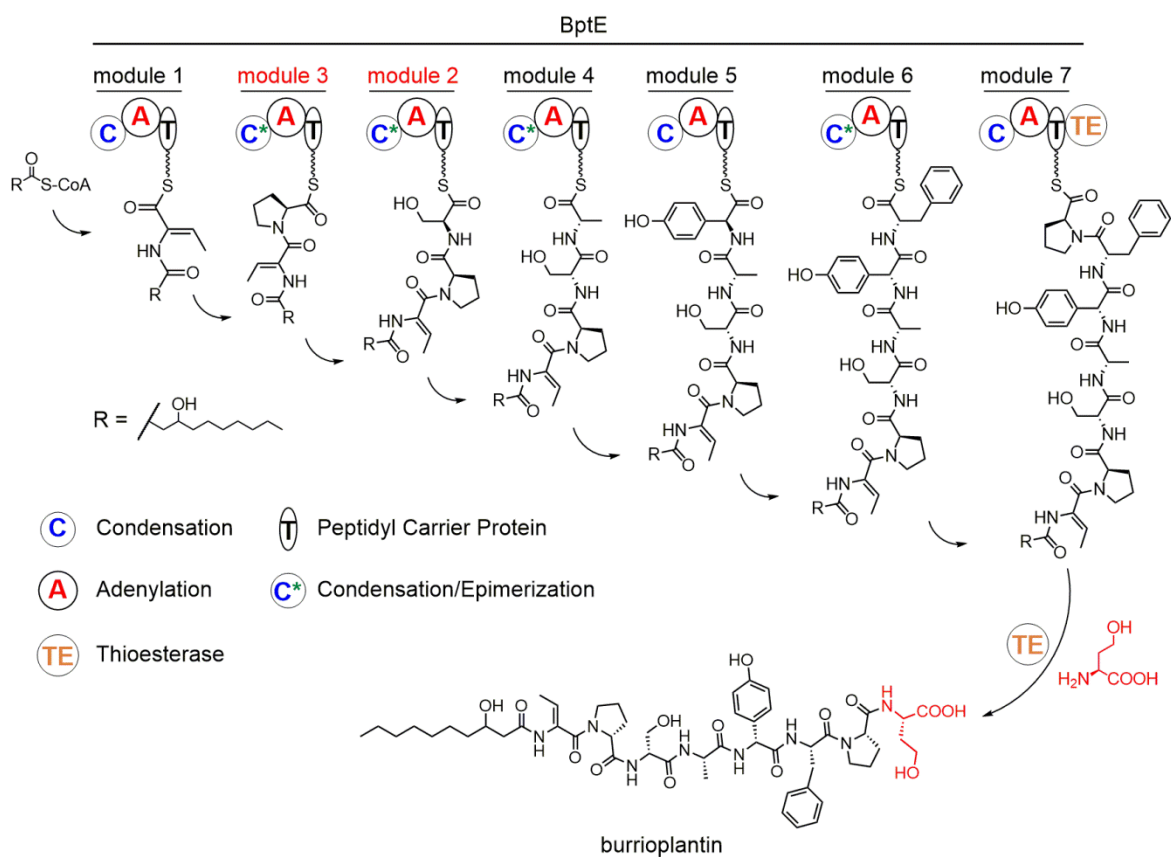
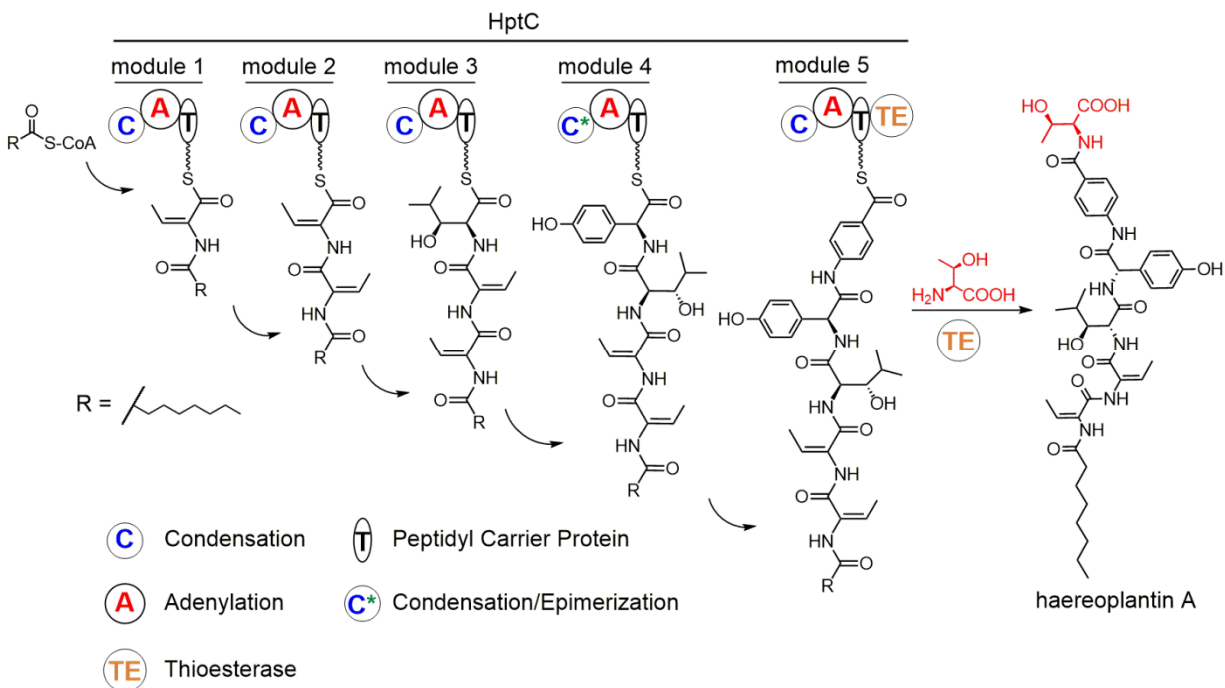


Figure S5. 800 MHz NMR spectra of gladiobactin in DMSO-*d*₆. Shown ¹H, ¹³C, COSY, HSQC, TOCSY, and HMBC spectra.

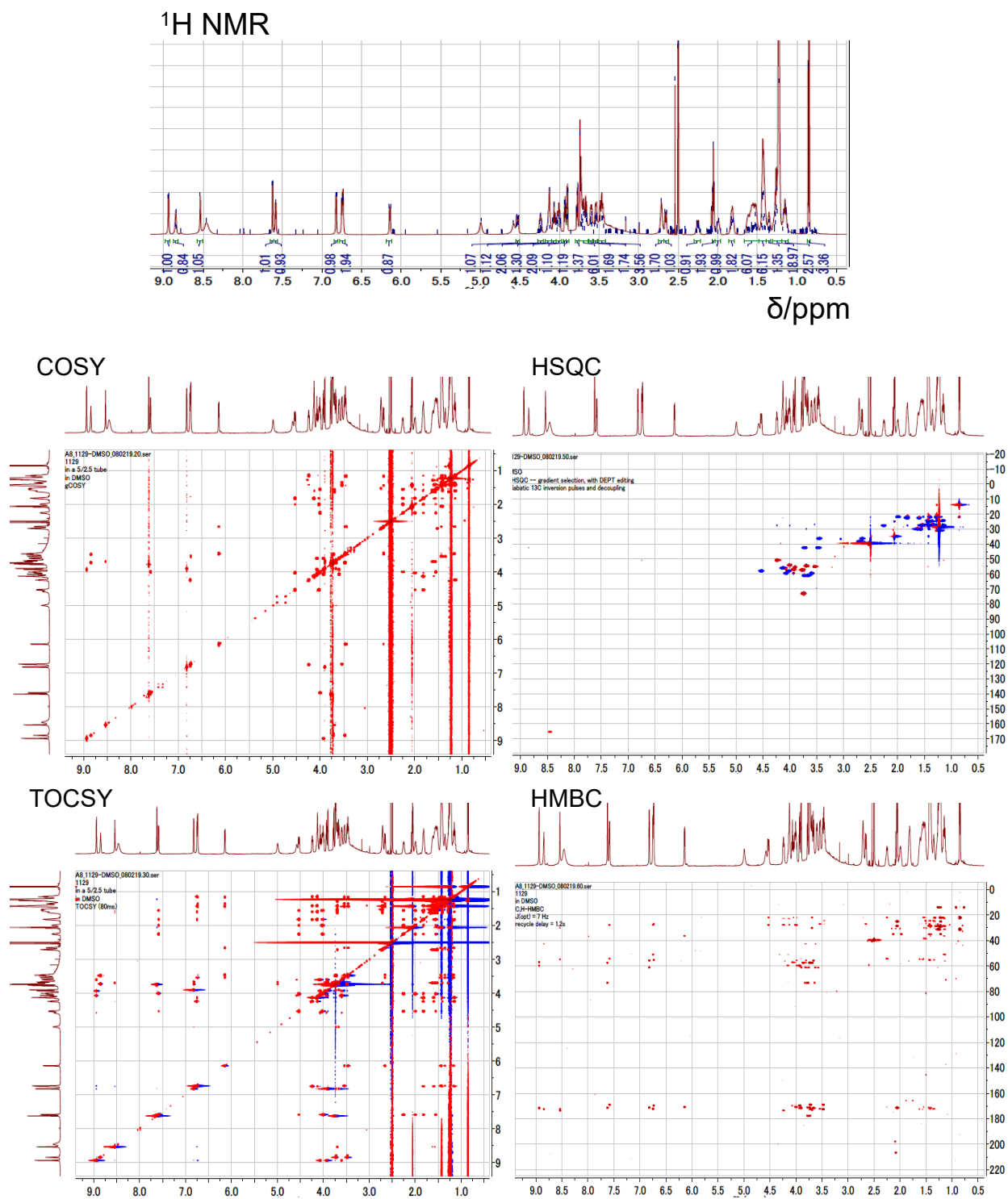


Figure S6. HR-MS/MS analysis of ferric-gladiobactin A. The loss of NO fragments is indicated.

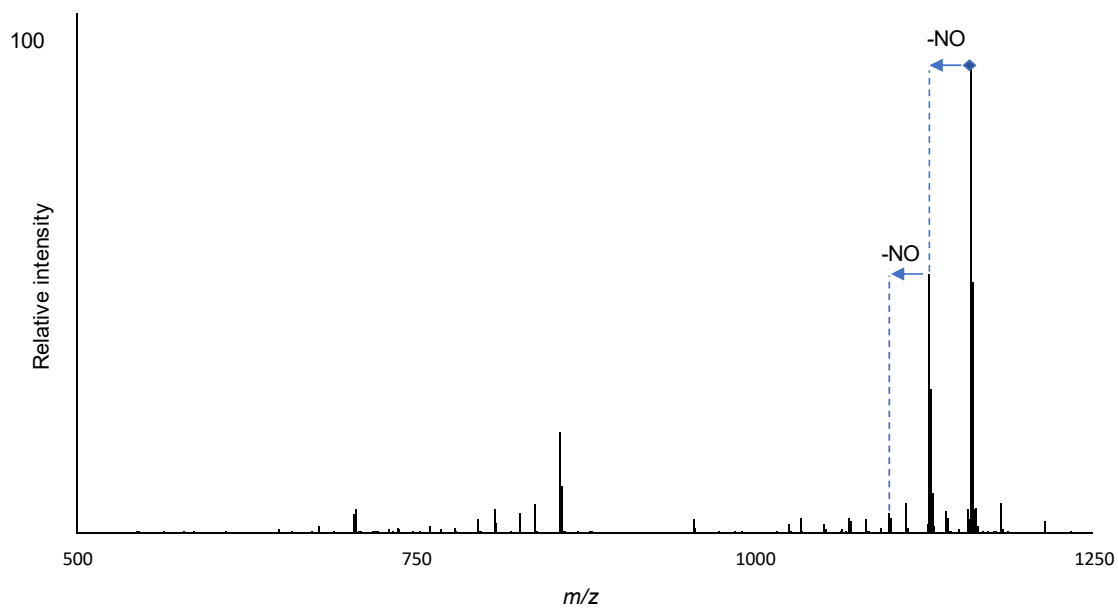
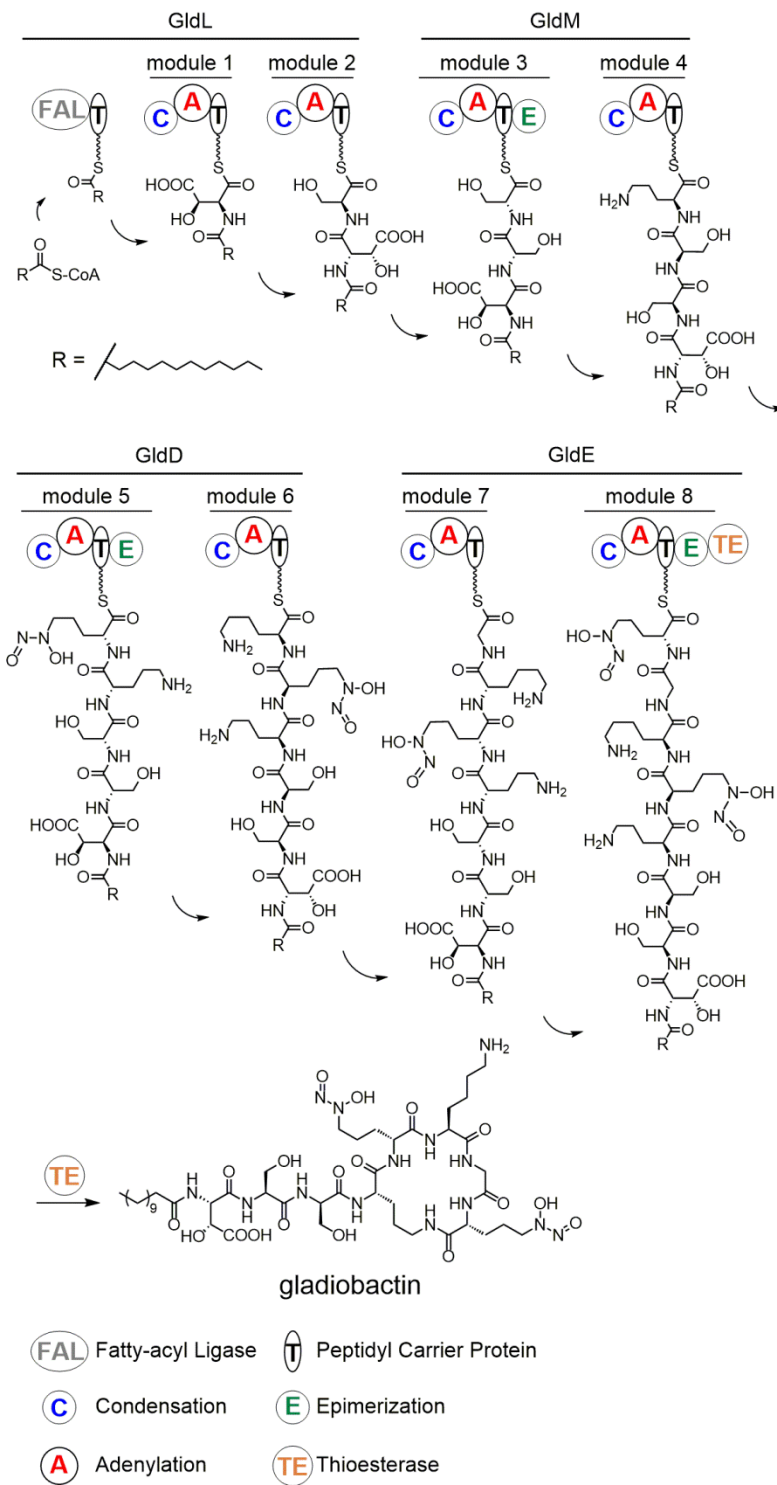


Figure S7. Proposed biosynthetic pathway for gladiobactin A. See Table S16.



SI References

- 1) Goryshin, I. Y., Jendrisak, J., Hoffman, L. M., Meis, R., and Reznikoff, W. S. (2000) Insertional transposon mutagenesis by electroporation of released Tn5 transposition complexes. *Nat. Biotechnol.* *18*, 97-100.
- 2) Goodwin, C. R., Covington, B. C., Derewacz, D. K., McNees, C. R., Wikswo, J. P., McLean, J. A., and Bachmann, B. O. (2015) Structuring microbial metabolic responses to multiplexed stimuli via self-organizing metabolomics maps. *Chem. Biol.* *22*, 661-670.
- 3) Xu, F., Wu, Y., Zhang, C., Davis, K. M., Moon, K., Bushin, L. B., and Seyedsayamdost, M. R. (2019) A genetics-free method for high-throughput discovery of cryptic microbial metabolites. *Nat. Chem. Biol.* *15*, 161-168.
- 4) Marfey, P. (1984) Determination of D-amino acids. II. Use of a bifunctional reagent, 1,5-difluoro-2,4-dinitrobenzene. *Carlsberg Res. Commun.* *49*, 591-596.
- 5) Wang, R., Gallant, É., and Seyedsayamdost, M. R. (2016) Investigation of the genetics and biochemistry of roseobacticide production in the Roseobacter clade *bacterium Phaeobacter inhibens*. *MBio* *7*, e02118-15.